Available online at www.sciencedirect.com
SCIENCE DIRECT®
ELSEVIER
Computer Aided Geometric Design 22 (2005) 551–565
COMPUTER AIDED GEOMETRIC DESIGN
www.elsevier.com/locate/cagd

Helix approximations with conic and quadratic Bézier curves

Young Joon Ahn

Department of Mathematics Education, Chosun University, Gwangju 501-759, South Korea

Received 10 August 2002; received in revised form 10 August 2002; accepted 22 February 2005

Available online 10 May 2005

Abstract

In this paper we present the error analysis for the approximation of a cylindrical helix by conic and quadratic Bézier curves. The approximation method yields G^1 conic spline and G^1 quadratic spline, respectively. We give a sharp upper bound of the Hausdorff distance between the helix and each approximation curve. We also show that the error bound has the approximation order three and monotone increases as the angle subtended to helix increases. Furthermore, using the error bound analysis for the helix approximation by conic and quadratic Bézier curves, we present the error bounds for the torus-like helicoid approximations by quadric surfaces and quadratic Bézier tensor product surfaces.

Keywords: Helix; Conic; Quadratic Bézier curve; Helicoid surface; Quadric surface; Quadratic Bézier surface; Hausdorff distance; G^1 interpolation

1. Introduction

Circular arcs are the plane curves with constant curvature, and helix segments are the spatial curves with constant curvature and constant torsion. Circular arcs are widely used in the fields of Computer Aided Geometric Design and Computer Graphics. Helices can be also used importantly in the fields, for the tool path description, the simulation of kinematic motion or the design of highways, etc. Since circular arcs cannot be represented by polynomials in explicit form, circular arc approximations with Bézier curves have been developed in many papers (Ahn and Kim, 1997; de Boor et al., 1987; Dokken et al., 1990; Floater, 1995, 1997; Goldapp, 1991; Mørken, 1990). Since helices cannot be represented

E-mail address: ahn@chosun.ac.kr (Y.J. Ahn).

0167-8396/$ – see front matter
doi:10.1016/j.cagd.2005.02.003

by polynomials or rational polynomials in explicit form, the helix approximations with rational Bézier curves have been also developed in many papers. They are focused on the rational Bézier curves of degree three (Jehásusz, 1995), of degree three and four (Mick and Röschel, 1990), or of degree from four to six (Seemann, 1997). Recently, Yang (2003) also proposed the method for helix approximation using quintic rational Bézier curves.

In this paper the helix is approximated by quadratic rational/polynomial Bézier curves. Since they are easy to be handled and have the ability to yield tangent continuous splines, they are widely used curves in CAD/CAM systems, e.g., to design the bodies of aircraft, to design the outlines of fonts (Ahn, 2002b; Pavlidis, 1983; Pratt, 1985) or to express circular arcs, spheres or tori (Piegl, 1986, 1987; Piegl and Tiller, 1987; Sederberg et al., 1985; Tiller, 1983; Wilson, 1987). Thus many papers (Ahn, 2001; Cox and Harris, 1990; Farin, 1989; Floater, 1995; Schaback, 1993) relevant to the approximations of plane curves or data by quadratic rational/polynomial Bézier curves were published. In this paper the error bound analysis for the helix approximation by the quadratic rational/polynomial Bézier curves is presented.

Using rotation and translation any cylindrical helix could be represented by

$$\mathbf{h}(\theta) = (r\cos\theta, r\sin\theta, p\theta), \quad \theta \in [-\alpha, \alpha], \tag{1}$$

for some positive real numbers α, p and r. In this paper a sharp upper bound of the Hausdorff distance between the helix and each approximation curve $\mathbf{p}(t)$, $t \in [a, b]$, is presented, where the Hausdorff distance is defined (Ahn, 2001; Degen, 1992; Floater, 1995) by

$$d_H(\mathbf{h}, \mathbf{p}) = \max\Big\{ \max_{-\alpha\leqslant\theta\leqslant\alpha} \min_{a\leqslant t\leqslant b} \big|\mathbf{h}(\theta) - \mathbf{p}(t)\big|, \max_{a\leqslant t\leqslant b} \min_{-\alpha\leqslant\theta\leqslant\alpha} \big|\mathbf{h}(\theta) - \mathbf{p}(t)\big| \Big\}.$$

All upper bounds of the Hausdorff distances we present are monotone increasing as α increases so that the subdivision schemes with equi-distance of the helix can be obtained and yield the G^1 quadratic rational/polynomial splines. Also the upper bounds are of approximation order three $\mathcal{O}(\alpha^3)$ which is optimal order of approximation (Degen, 1992, 1993; Höllig and Koch, 1995, 1996) with spatial quadratic rational/polynomial Bézier curves.

We also approximate the torus-like helicoid by quadric surfaces and quadratic Bézier tensor-product surfaces. An upper bound of the Hausdorff distance between the torus-like helicoid and each approximation surface is presented in explicit form. In particular, the error bound analysis for the helix or the helicoid approximations with the quadratic polynomial curves and surfaces are well done by the help of Floater's error analysis (Floater, 1995), which is restated in Proposition 2 in this paper.

The paper is organized as follows. In Section 2, the helix approximations with conic and quadratic Bézier curves are presented. In Section 3, the torus-like helicoid approximations with quadric surfaces and quadratic Bézier surfaces are given. In Section 4, our approximation method is applied to some examples. In Section 5, we summarize our work.

2. Helix approximations with quadratic rational and polynomial curves

In this section the helix in Eq. (1) for $0 < \alpha < \pi/2$ is approximated by quadratic rational/polynomial Bézier curves

$$\mathbf{r}(t) = \frac{\sum_{i=0}^{2} w_i \mathbf{b}_i B_i(t)}{\sum_{i=0}^{2} w_i B_i(t)}, \quad 0 \leqslant t \leqslant 1,$$

$$\mathbf{q}(u) = \sum_{i=0}^{2} \mathbf{b}_i B_i(u), \quad 0 \leqslant u \leqslant 1,$$

having the control points

$$\begin{aligned}
\mathbf{b}_0 &= (x_0, y_0, z_0) = (r\cos\alpha, -r\sin\alpha, -p\alpha),\\
\mathbf{b}_1 &= (x_1, y_1, z_1) = (r\sec\alpha, 0, 0),\\
\mathbf{b}_2 &= (x_2, y_2, z_2) = (r\cos\alpha, r\sin\alpha, p\alpha)
\end{aligned}$$

and the weights $w_0 = 1$, $w_1 = \cos\alpha$, $w_2 = 1$, as shown in Fig. 1, where $B_i(t) = \binom{2}{i} t^i (1-t)^{2-i}$, $i = 0, 1, 2$, is the quadratic Bernstein polynomial. Since the weight $\cos\alpha$ is less than one, the conic $\mathbf{r}(t)$ is an ellipse segment (Ahn and Kim, 1998; Farin, 1998; Lee, 1987). The helix lies on the cylinder $x^2 + y^2 = r^2$, and all points of $\mathbf{r}(t)$ and two end points $\mathbf{q}(0)$ and $\mathbf{q}(1)$ of $\mathbf{q}(u)$ lie on the cylinder. Also three points of $\mathbf{r}(t)$, $t = 0, 1/2, 1$, and two points $\mathbf{q}(0)$ and $\mathbf{q}(1)$ are on the helix. Note that although both approximation curves $\mathbf{r}(t)$ and $\mathbf{q}(u)$ are G^0 end points interpolations of the helix, the approximations by the quadratic rational/polynomial curves for each subdivided segment of the helix with equi-length yield G^1 quadratic rational/polynomial splines. Putting

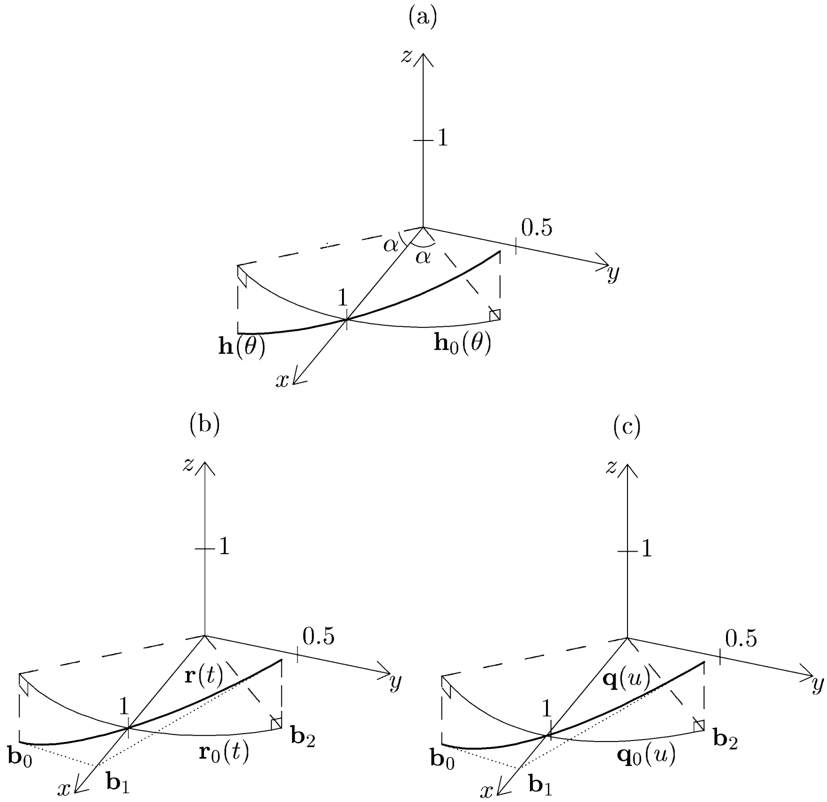

Fig. 1. (a) The helix $\mathbf{h}(\theta) = (r\cos\theta, r\sin\theta, p\theta)$, $\theta \in [-\alpha, \alpha]$, and its projection $\mathbf{h}_0(\theta)$ on xy-plane, when $p = r = 1$ and $\alpha = \pi/4$. (b) The conic approximation $\mathbf{r}(t)$, $t \in [0, 1]$, and its projection $\mathbf{r}_0(t)$. (c) The quadratic Bézier approximation $\mathbf{q}(u)$, $u \in [0, 1]$, and its projection $\mathbf{q}_0(u)$. The dotted lines are control polygon $\mathbf{b}_0\mathbf{b}_1\mathbf{b}_2$.

$$w(t) = \sum_{i=0}^{2} w_i B_i(t) = (1-t)^2 + 2\cos\alpha t(1-t) + t^2,$$

$$x(t) = \sum_{i=0}^{2} w_i x_i B_i(t) = r\left(\cos\alpha(1-t)^2 + 2t(1-t) + \cos\alpha t^2\right),$$

$$y(t) = \sum_{i=0}^{2} w_i y_i B_i(t) = r\sin\alpha(2t-1),$$

$$z(t) = \sum_{i=0}^{2} w_i z_i B_i(t) = p\alpha(2t-1),$$

we have

$$\mathbf{r}(t) = \big(x(t), y(t), z(t)\big)/w(t), \qquad \text{for } t \in [0,1]. \tag{2}$$

Remark 1. In particular, for $p = 0$, let the curves $\mathbf{h}(\theta)$, $\mathbf{r}(t)$ and $\mathbf{q}(u)$ be denoted by $\mathbf{h}_0(\theta)$, $\mathbf{r}_0(t)$ and $\mathbf{q}_0(u)$, respectively, as shown in Fig. 1. Then $\mathbf{h}_0(\theta)$ and $\mathbf{r}_0(t)$ are the same circular arc with angle 2α on xy-plane. Also, each point of the helix $\mathbf{h}(\theta)$ is obtained by translation of each point of the circular arc $\mathbf{h}_0(\theta)$ by $p\theta$ in the direction of z-axis. The quadratic rational Bézier approximation $\mathbf{r}(t)$ also has the control points obtained by translation of the control points of $\mathbf{r}_0(t)$ by $-p\alpha$, 0, $p\alpha$, in order, along the z-axis.

The following proposition was presented by Floater (1995), which is needed to analyze the error bounds proposed in this paper.

Proposition 2. *Let a conic $\mathbf{r}(t)$ and a quadratic Bézier curve $\mathbf{q}(u)$ have the same control points $\mathbf{p}_0, \mathbf{p}_1, \mathbf{p}_2$, and $\mathbf{r}(t)$ have the weights 1, w, 1, in order. Then there is a reparametrisation (or one-to-one and onto mapping) $t(u)$ such that $\mathbf{r}(t(u)) - \mathbf{q}(u)$ is parallel with $\mathbf{p}_0 - 2\mathbf{p}_1 + \mathbf{p}_2$ and*

$$\left|\mathbf{r}\big(t(u)\big) - \mathbf{q}(u)\right| \leqslant \frac{|1-w|}{4(1+w)} |\mathbf{p}_0 - 2\mathbf{p}_1 + \mathbf{p}_2|.$$

Proof. See Proposition 2.1 and Corollary 2.2 in (Floater, 1995). □

We analyze the error bound of the helix approximation with the quadratic rational/polynomial Bézier curves. In the following proposition, the upper bounds of the Hausdorff distances $d_H(\mathbf{h}, \mathbf{r})$ and $d_H(\mathbf{h}, \mathbf{q})$ are presented.

Proposition 3. *For each α, p and r, the helix approximations with the quadratic rational/polynomial curves have the error bounds*

$$d_H(\mathbf{h}, \mathbf{r}) \leqslant pE(\alpha), \tag{3}$$

$$d_H(\mathbf{h}, \mathbf{q}) \leqslant \sqrt{\big(pE(\alpha)\big)^2 + \big(rF(\alpha)\big)^2}, \tag{4}$$

where

$$t_A = \frac{1}{2} - \frac{1}{2}\sqrt{\frac{(1+\cos\alpha)(\alpha-\sin\alpha)}{(1-\cos\alpha)(\alpha+\sin\alpha)}},$$

$$E(\alpha) = \arctan\frac{y(t_A)}{x(t_A)} - \frac{z(t_A)}{pw(t_A)},$$

$$F(\alpha) = 2\sin^4\frac{\alpha}{2}\sec\alpha.$$

Proof. It is well known (Ahn, 2001, 2002a; Floater, 1995, 1997) that

$$d_H(\mathbf{h},\mathbf{r}) \leqslant \max_{0\leqslant t\leqslant 1}\big|\mathbf{h}\big(\theta(t)\big) - \mathbf{r}(t)\big| \tag{5}$$

for a reparametrisation (or one-to-one and onto mapping) $\theta = \theta(t)$. With the reparametrisation $\theta = \arctan(y(t)/x(t))$, Eqs. (1) and (2) yield

$$\mathbf{h}\big(\theta(t)\big) - \mathbf{r}(t) = \left(\frac{rx}{\sqrt{x^2+y^2}}, \frac{ry}{\sqrt{x^2+y^2}}, p\arctan\frac{y}{x}\right) - \left(\frac{x}{w}, \frac{y}{w}, \frac{z}{w}\right).$$

Since $x(t)^2 + y(t)^2 = r^2 w(t)^2$, we have

$$\mathbf{h}\big(\theta(t)\big) - \mathbf{r}(t) = \left(0, 0, p\arctan\frac{y(t)}{x(t)} - \frac{z(t)}{w(t)}\right).$$

The third component of the last equation is denoted by $\varepsilon(t)$. Its derivative is

$$\varepsilon'(t) = p\frac{y'x - yx'}{x^2+y^2} - \frac{z'w - zw'}{w^2} = \frac{p(y'x-yx') - r^2(z'w - zw')}{r^2w^2}.$$

The numerator of $\varepsilon'(t)$ in the last equation is the quadratic polynomial

$$2pr^2\big\{2(\alpha+\sin\alpha)(1-\cos\alpha)(t^2-t) + (\sin\alpha - \alpha\cos\alpha)\big\}$$

and has zeros at

$$t_A = \frac{1}{2} - \frac{1}{2}\sqrt{\frac{(1+\cos\alpha)(\alpha-\sin\alpha)}{(1-\cos\alpha)(\alpha+\sin\alpha)}}, \qquad t_B = \frac{1}{2} + \frac{1}{2}\sqrt{\frac{(1+\cos\alpha)(\alpha-\sin\alpha)}{(1-\cos\alpha)(\alpha+\sin\alpha)}}.$$

Since $(1+\cos\alpha)(\alpha-\sin\alpha) < (1-\cos\alpha)(\alpha+\sin\alpha)$, both zeros lie in the open interval $(0,1)$, as shown in Fig. 2(a). Since $\varepsilon(t) = 0$ for $t = 0, 1/2, 1$, and $\varepsilon'(t)$ is positive in $(0, t_A)$ and $(t_B, 1)$, $\varepsilon(t)$ has the local maximum $\varepsilon(t_A)$ and the local minimum $\varepsilon(t_B)$ and $\varepsilon(t_A) = -\varepsilon(t_B)$ is the global maximum of $\varepsilon(t)$ in the closed interval $[0,1]$, as shown in Fig. 2(b).

With the reparametrisation $\theta = \arctan(y(t)/x(t))$, $\mathbf{h}(\theta) - \mathbf{r}(t)$ is parallel to z-axis, and

$$\big|\mathbf{h}(\theta) - \mathbf{r}(t)\big| \leqslant \varepsilon(t_A) = p\left(\arctan\frac{y(t_A)}{x(t_A)} - \frac{z(t_A)}{pw(t_A)}\right) = pE(\alpha) \tag{6}$$

for all $0 \leqslant t \leqslant 1$. Thus the upper bound (3) follows from Eqs. (5)–(6).

Now, we find an upper bound of the Hausdorff distance $d_H(\mathbf{h},\mathbf{q})$ between the helix $\mathbf{h}(\theta)$ and the quadratic Bézier approximation $\mathbf{q}(u)$. Since $\mathbf{q}(u)$ and $\mathbf{r}(t)$ have the same control points $\mathbf{b}_0, \mathbf{b}_1, \mathbf{b}_2$, by

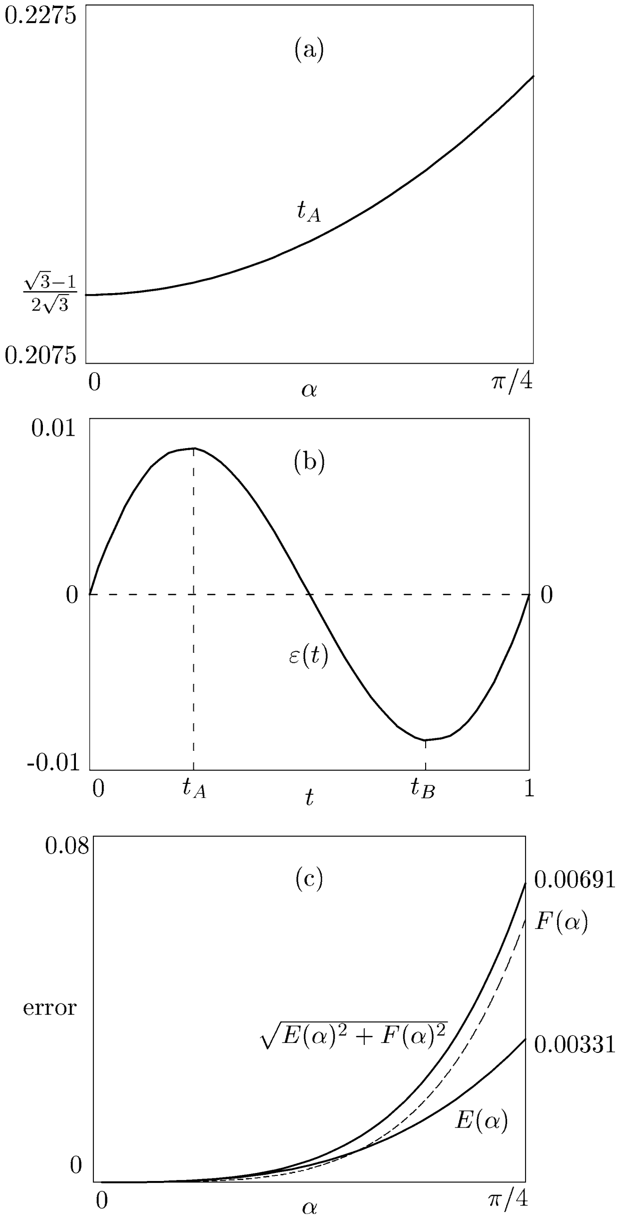

Fig. 2. (a) t_A for $\alpha \in [0, \pi/4]$. (b) $\varepsilon(t)$ for $t \in [0, 1]$ when $\alpha = \pi/4$. (c) The upper bounds $pE(\alpha)$ and $\sqrt{p^2E(\alpha)^2 + r^2F(\alpha)^2}$ (solid lines) with $F(\alpha)$ (dash lines) for $\alpha \in [0, \pi/4]$ when $p = r = 1$.

Proposition 2, there exists a reparametrisation $t = t(u)$ such that $\mathbf{r}(t(u)) - \mathbf{q}(u)$ is parallel with $\mathbf{b}_0 - 2\mathbf{b}_1 + \mathbf{b}_2$ and

$$\left|\mathbf{r}\bigl(t(u)\bigr) - \mathbf{q}(u)\right| \leqslant \frac{1 - \cos\alpha}{4(1 + \cos\alpha)} |\mathbf{b}_0 - 2\mathbf{b}_1 + \mathbf{b}_2|.$$

The vector $\mathbf{b}_0 - 2\mathbf{b}_1 + \mathbf{b}_2 = -2r(\sin^2\alpha\sec\alpha, 0, 0)$ is parallel with x-axis, and

$$\begin{aligned}\big|\mathbf{r}\big(t(u)\big) - \mathbf{q}(u)\big| &\leqslant \frac{(1-\cos\alpha)}{4(1+\cos\alpha)} \times 2r\sin^2\alpha\sec\alpha \\ &= 2r\sin^4\frac{\alpha}{2}\sec\alpha = rF(\alpha).\end{aligned}$$

Thus for all $u \in [0, 1]$, with the reparametrisation $\theta = \theta(t(u))$

$$\begin{aligned}\big|\mathbf{h}(\theta) - \mathbf{q}(u)\big| &= \Big|\Big(\mathbf{h}\big(\theta\big(t(u)\big)\big) - \mathbf{r}\big(t(u)\big)\Big) + \Big(\mathbf{r}\big(t(u)\big) - \mathbf{q}(u)\Big)\Big| \\ &\leqslant \big|\pm p\big(0, 0, E(\alpha)\big) + r\big(F(\alpha), 0, 0\big)\big| \\ &= \sqrt{p^2E(\alpha)^2 + r^2F(\alpha)^2}.\end{aligned}$$

Hence we obtain the upper bound (4). □

As an illustration, for the given helix $\mathbf{h}(\theta) = (\cos\theta, \sin\theta, \theta)$, $\theta \in [-\pi/4, \pi/4]$, we obtain the conic and the quadratic Bézier approximations as shown in Figs. 1(b)–(c). By the proposition above, the upper bounds of $d_H(\mathbf{h}, \mathbf{r})$ and $d_H(\mathbf{h}, \mathbf{q})$ are 3.31×10^{-2} and 6.91×10^{-2}, respectively. We also find the real Hausdorff distances $d_H(\mathbf{h}, \mathbf{r}) = 2.35 \times 10^{-2}$ and $d_H(\mathbf{h}, \mathbf{q}) = 6.07 \times 10^{-2}$, numerically. Although our error bounds are larger than the real Hausdorff distances, our error bounds are obtainable in explicit form, and the real Hausdorff distances induce high computational complexities to find.

It is clear that $F(\alpha)$ is a strictly increasing function and has the approximation order four $\mathcal{O}(\alpha^4)$. In the following proposition, verifying that $E(\alpha)$ is strictly increasing and is of approximation order three $\mathcal{O}(\alpha^3)$, we can see that the upper bounds of the Hausdorff distances $d_H(\mathbf{h}, \mathbf{r})$ and $d_H(\mathbf{h}, \mathbf{q})$ are also strictly increasing and are of approximation order three.

Proposition 4. *The error bounds of $d_H(\mathbf{h}, \mathbf{r})$ and $d_H(\mathbf{h}, \mathbf{q})$ are monotone increasing as α increases and have approximation order three $\mathcal{O}(\alpha^3)$.*

Proof. See Appendix A. □

Put $f(\alpha) = \sqrt{(pE(\alpha))^2 + (rF(\alpha))^2}$. Then $E(\alpha)$ and $f(\alpha)$ are increasing functions, and so the inverse functions E^{-1} and f^{-1} exist, as shown in Fig. 2(c). Using the fact, we have a subdivision scheme for helix approximation with the conic and the quadratic Bézier curves within tolerance.

Corollary 5. *Let a tolerance τ be given. The piece-wise approximation of the conic and quadratic Bézier curves are achieved within the tolerance τ, by subdividing the helix with equi-distance into k-pieces*

$$k = \big\lceil \alpha p/E^{-1}(\tau)\big\rceil \quad \textit{and} \quad \big\lceil \alpha/f^{-1}(\tau)\big\rceil$$

respectively, where $\lceil \mathrm{x} \rceil$ *is the smallest integer larger than or equal to* x.

Also, we present the subdivision algorithm searching for the minimum number of pieces within tolerance as stated in Corollary 5. We denote the upper bound of the Hausdorff distance $d_H(\mathbf{h}, \mathbf{r})$ and $d_H(\mathbf{h}, \mathbf{q})$ in Proposition 3 by $\psi(p, r, \alpha)$.

Algorithm.
input p, r, α, τ

$k_{\min} \Leftarrow 0$
$k_{\max} \Leftarrow 1$
$\alpha_0 \Leftarrow \alpha$
while $\alpha_0 \geqslant \pi/2$ or $\psi(p, r, \alpha_0) > \tau$ **do**
  $k_{\min} \Leftarrow k_{\max}$
  $k_{\max} \Leftarrow 2 \times k_{\max}$
  $\alpha_0 \Leftarrow \alpha / k_{\max}$
end do
while $k_{\max} - k_{\min} > 1$ **do**
  $k \Leftarrow (k_{\max} + k_{\min})/2$
  $\alpha_0 \Leftarrow \alpha / k;$
  if $\alpha_0 < \pi/2$ or $\psi(p, r, \alpha_0) < \tau$
    then $k_{\max} \Leftarrow k$
    else $k_{\min} \Leftarrow k$
end do

output $k_{\max}$

3. Torus-like helicoid approximations

Let the 'torus-like helicoid' $\mathbf{H}(\theta, \phi)$ be defined by

$$\mathbf{H}(\theta, \phi) = \big((r + \rho\cos\phi)\cos\theta, (r + \rho\cos\phi)\sin\theta, \rho\sin\phi + p\theta\big)$$

for the rectangular domain $(\theta, \phi) \in [-\alpha, \alpha] \times [\beta_1 - \beta, \beta_1 + \beta]$. Note that the surface $\mathbf{H}(\theta, \phi)$ is circular helix in θ and circular arc in ϕ. The surface $\mathbf{H}(\theta, \phi)$ when $p = 0$ is denoted by $\mathbf{H}_0(\theta, \phi)$, which is a patch of torus. Let the torus-like helicoid approximation with the quadratic rational/polynomial tensor-product surfaces be denoted by $R(t, s)$ and $Q(u, v)$, respectively. For $0 < \alpha < \pi/2$, we define the quadratic rational/polynomial Bézier surface approximations

$$R(t, s) = \frac{\sum_{i=0}^{2}\sum_{j=0}^{2} w_{ij}\mathbf{b}_{ij}B_i(t)B_j(s)}{\sum_{i=0}^{2}\sum_{j=0}^{2} w_{ij}B_i(t)B_j(s)}, \quad (t, s) \in [0, 1] \times [0, 1],$$

$$Q(u, v) = \sum_{i=0}^{2}\sum_{j=0}^{2}\mathbf{b}_{ij}B_i(t)B_j(s), \quad (u, v) \in [0, 1] \times [0, 1],$$

having the control points

$$\mathbf{b}_{00} = \big((r + \rho\cos\beta_0)\cos\alpha, -(r + \rho\cos\beta_0)\sin\alpha, \rho\sin\beta_0 - p\alpha\big),$$
$$\mathbf{b}_{01} = \big((r + \rho\sec\beta\cos\beta_1)\cos\alpha, -(r + \rho\sec\beta\cos\beta_1)\sin\alpha, \rho\sec\beta\sin\beta_1 - p\alpha\big),$$
$$\mathbf{b}_{02} = \big((r + \rho\cos\beta_2)\cos\alpha, -(r + \rho\cos\beta_2)\sin\alpha, \rho\sin\beta_2 - p\alpha\big),$$

$$\mathbf{b}_{10} = \big((r + \rho\cos\beta_0)\sec\alpha, 0, \rho\sin\beta_0\big),$$
$$\mathbf{b}_{11} = \big((r + \rho\sec\beta\cos\beta_1)\sec\alpha, 0, \rho\sec\beta\sin\beta_1\big),$$
$$\mathbf{b}_{12} = \big((r + \rho\cos\beta_2)\sec\alpha, 0, \rho\sin\beta_2\big),$$
$$\mathbf{b}_{20} = \big((r + \rho\cos\beta_0)\cos\alpha, (r + \rho\cos\beta_0)\sin\alpha, \rho\sin\beta_0 + p\alpha\big),$$
$$\mathbf{b}_{21} = \big((r + \rho\sec\beta\cos\beta_1)\cos\alpha, (r + \rho\sec\beta\cos\beta_1)\sin\alpha, \rho\sec\beta\sin\beta_1 + p\alpha\big),$$
$$\mathbf{b}_{22} = \big((r + \rho\cos\beta_2)\cos\alpha, (r + \rho\cos\beta_2)\sin\alpha, \rho\sin\beta_2 + p\alpha\big),$$

where $\beta_0 = \beta_1 - \beta$ and $\beta_2 = \beta_1 + \beta$, and the weights

$$(w_{ij}) = \begin{pmatrix} 1 & \cos\beta & 1 \\ \cos\alpha & \cos\alpha\cos\beta & \cos\alpha \\ 1 & \cos\beta & 1 \end{pmatrix}.$$

Note that $R(t,s)$ is conic in t and circular arc in s, and $Q(u,v)$ are quadratic Bézier curves in u and v, respectively. Let $R(t,s)$ when $p = 0$ be denoted by $R_0(t,s)$. Then $\mathbf{H}_0(\theta,\phi)$ and $R_0(s,t)$ are the same patch of torus.

Proposition 6. *For each α, β, p, r and ρ, the torus-like helicoid approximations with the quadratic rational/polynomial tensor-product surfaces have the error bounds*

$$d_H(\mathbf{H}, R) \leqslant pE(\alpha), \tag{7}$$
$$d_H(\mathbf{H}, Q) \leqslant \sqrt{\big(pE(\alpha)\big)^2 + \big((r+\rho)F(\alpha)\big)^2} + \frac{\rho F(\beta)}{\cos\alpha}. \tag{8}$$

Proof. Since both surface $\mathbf{H}_0(\theta,\phi)$ and $R_0(t,s)$ are the same torus, there exist reparametrisations $\theta(t)$ and $\phi(s)$ such that

$$\mathbf{H}_0\big(\theta(t),\phi(s)\big) = R_0(t,s)$$

for $(t,s) \in [0,1] \times [0,1]$. For each fixed $s_0 \in [0,1]$, with $\phi_0 = \phi(s_0)$, the two isoparametric curves $\mathbf{H}_0(\theta,\phi_0)$ and $R_0(t,s_0)$ are on the same circle

$$x^2 + y^2 = (r + \rho\cos\phi_0)^2, \qquad z = \rho\sin\phi_0.$$

Note that the curve $\mathbf{H}(\theta,\phi_0)$ is the helix whose points are obtained by translation of the circular arc $\mathbf{H}_0(\theta,\phi_0)$ by $p\theta$, $\theta \in [-\alpha,\alpha]$, in the direction of z-axis, and $R(t,s_0)$ is the quadratic rational Bézier curve having the control points obtained by translation of the control points of $R_0(t,s_0)$ by $-p\alpha$, 0 and $p\alpha$ in order, along z-axis, as stated in Remark 1. Thus $R(t,s_0)$ is the conic approximation of the helix $\mathbf{H}(\theta,\phi_0)$ using the same method proposed in Section 2. Hence, by the error analysis in Proposition 3, for each $s \in [0,1]$ and each $t \in [0,1]$, with the reparametrisations $\theta = \theta(t)$ and $\phi = \phi(s)$, $\mathbf{H}(\theta,\phi) - R(t,s)$ is parallel to z-axis and $|\mathbf{H}(\theta,\phi) - R(t,s)| \leqslant pE(\alpha)$ which is independent of the radius $r + \rho\cos\phi_0$ of the circle. Thus we have the error bound (7) clearly.

Now, we find the upper bound (8) of the Hausdorff distance between $\mathbf{H}(\theta,\phi)$ and $Q(u,v)$. At first, we find an upper bound of the Hausdorff distance $d_H(R,Q)$ between $R(t,s)$ and $Q(u,v)$, by the help of the method of error bound analysis proposed by Floater (1995). Let the intermediate surface $P(u,s)$ be defined by

$$P(u,s) = \frac{\sum_{i=0}^{2}\sum_{j=0}^{2} B_i(u)B_j(s)w_{0j}\mathbf{b}_{ij}}{\sum_{j=0}^{2} B_j(s)w_{0j}}$$

which is rational (circular arc) in s but non-rational (quadratic Bézier curve) in u. Then for each fixed $s_0 \in [0,1]$ with $\phi_0 = \phi(s_0)$ two isoparametric curves $R(t,s_0)$ and $P(u,s_0)$ are the quadratic rational and polynomial Bézier curves having the same control points. Thus $P(u,s_0)$ is also the quadratic Bézier-interpolation of the isoparametric helix $\mathbf{H}(\theta,\phi_0)$ which is the same approximation method proposed in Section 2. By Proposition 3, we have for all $s_0 \in [0,1]$ with $\phi_0 = \phi(s_0)$

$$d_H\big(\mathbf{H}(\theta,\phi_0), P(u,s_0)\big) \leqslant \sqrt{\big(pE(\alpha)\big)^2 + \big((r+\rho\cos\phi_0)F(\alpha)\big)^2}$$

so that

$$d_H(\mathbf{H},P) \leqslant \sqrt{\big(pE(\alpha)\big)^2 + \big((r+\rho)F(\alpha)\big)^2}. \tag{9}$$

By Eqs. (10)–(11) in (Floater, 1995), the Hausdorff distance $d_H(P,Q)$ between the intermediate surface $P(u,s)$ and the quadratic Bézier surface $Q(u,v)$ has the upper bound

$$\big|P(u,s) - Q(u,v)\big| \leqslant \frac{1-\cos\beta}{4(1+\cos\beta)} \max_{i=0,1,2} |\mathbf{b}_{i0} - 2\mathbf{b}_{i1} - \mathbf{b}_{i2}|.$$

By simple calculations

$$|\mathbf{b}_{10} - 2\mathbf{b}_{11} + \mathbf{b}_{12}| = 2\rho\sin^2\beta\sec\beta\sqrt{\sin^2\beta_1 + \cos^2\beta_1\sec^2\alpha}$$

is larger than

$$|\mathbf{b}_{i0} - 2\mathbf{b}_{i1} + \mathbf{b}_{i2}| = 2\rho\sin^2\beta\sec\beta, \qquad i = 0,2.$$

It follows from $\sqrt{\sin^2\beta_1 + \cos^2\beta_1\sec^2\alpha} \leqslant 1/\cos\alpha$ that

$$\big|P(u,s) - Q(u,v)\big| \leqslant \frac{1-\cos\beta}{4(1+\cos\beta)} \times \frac{2\rho\sin^2\beta\sec\beta}{\cos\alpha} = \frac{\rho F(\beta)}{\cos\alpha}$$

and thus

$$d_H(P,Q) \leqslant \frac{\rho F(\beta)}{\cos\alpha}. \tag{10}$$

Since $d_H(\mathbf{H},Q) \leqslant d_H(\mathbf{H},P) + d_H(P,Q)$, Eqs. (9)–(10) yield the error bound (8). □

4. Examples

In this section the helix and the torus-like helicoid are approximated by the quadratic rational/polynomial curves/surfaces. Let the helix be given by

$$\mathbf{h}(\theta) = (r\cos\theta, r\sin\theta, p\theta), \quad \theta \in [0, 2\pi],$$

for $r = p = 1$, as shown in Fig. 3(a). Using the approximation method proposed in Section 2, we obtain the G^1 quadratic rational/polynomial spline curves $\mathbf{r}(t)$ and $\mathbf{q}(u)$ which are consisted of ‘four’ segments, respectively, as shown in Figs. 3(b)–(c). From Proposition 3 each error bounds are as follows

$$d_H(\mathbf{h},\mathbf{r}) \leqslant 0.0331 \quad \text{and} \quad d_H(\mathbf{h},\mathbf{q}) \leqslant 0.0691.$$

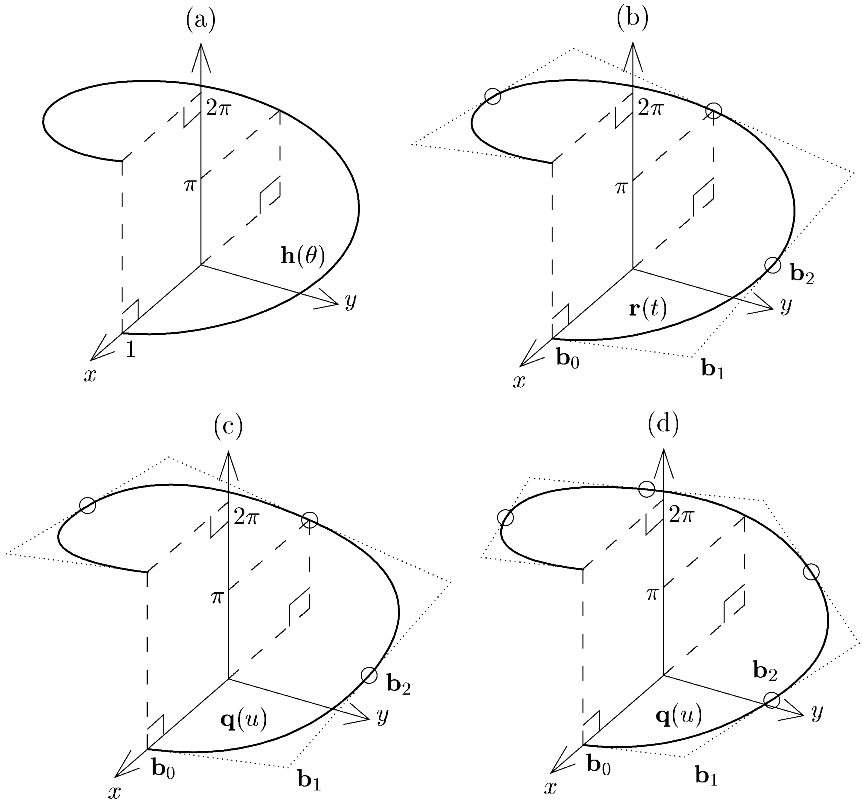

Fig. 3. (a) Helix curve $\mathbf{h}(\theta) = (\cos\theta, \sin\theta, \theta)$, $\theta \in [0, 2\pi]$. (b) Conic approximation $\mathbf{r}(t)$. (c)–(d) Quadratic Bézier curve $\mathbf{q}(u)$ using four and five segments. (b)–(d) The dotted lines are control polygons. The circles are the junction points of two consecutive segments.

Table 1
The error bounds of $d_H(\mathbf{h}, \mathbf{r})$ and $d_H(\mathbf{h}, \mathbf{q})$ for the given helix curve $\mathbf{h}(\theta) = (\cos\theta, \sin\theta, \theta)$, $\theta \in [0, 2\pi]$, with k-segments, $k = 4, 8, 16$, and 32

No. segments	$d_H(\mathbf{h}, \mathbf{r})$	$d_H(\mathbf{h}, \mathbf{q})$
4	3.31×10^{-2}	6.91×10^{-2}
8	3.95×10^{-3}	5.04×10^{-3}
16	4.87×10^{-4}	5.23×10^{-4}
32	6.08×10^{-5}	6.18×10^{-5}

Also, the error bounds for the approximations of the helix by k-segments of $\mathbf{r}(t)$ and $\mathbf{q}(u)$, with $k = 8, 16, 32$, are obtained as shown in Table 1. We can see that the approximation order of these approximation methods are three $\mathcal{O}(\alpha^3)$.

Let tolerance be given by 0.05. Then the subdivision is not needed any more for the helix approximation by the conic $\mathbf{r}(t)$. Using the subdivision scheme in Corollary 5, the helix approximation by the quadratic $\mathbf{q}(u)$ can be achieved within the tolerance by the number of segments $k = 5$, as shown in

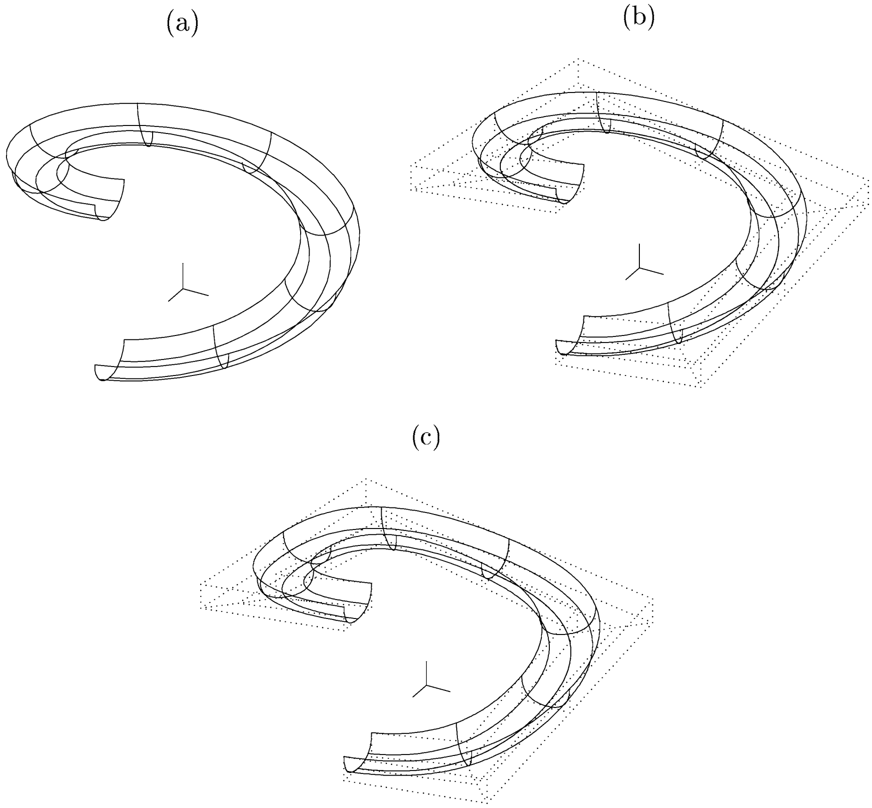

Fig. 4. (a) The torus-like helicoid surface $\mathbf{H}(\theta,\phi)$, $(\theta,\phi) \in [0,2\pi] \times [0,\pi]$ when $p=\rho=1$ and $r=5$. (b) The quadric surface approximation $R(t,s)$. (c) The quadratic Bézier surface $Q(u,v)$. (b)–(c) Using 4×2-patches. The dotted lines are control nets.

Fig. 3(d). They have the new upper bounds of the Hausdorff distances $d_H(\mathbf{h},\mathbf{q}) \leqslant 2.80 \times 10^{-2}$, which are less than the tolerance.

The second example is the torus-like helicoid approximations. Let $\mathbf{H}(\theta,\phi)$ be the helicoid given by

$$\mathbf{H}(\theta,\phi) = \bigl((r+\rho\cos\phi)\cos\theta, (r+\rho\cos\phi)\sin\theta, \rho\sin\phi + p\theta\bigr)$$

$(\theta,\phi) \in [0,2\pi] \times [0,\pi]$, for $r=5$ and $\rho=p=1$, as shown in Fig. 4(a). The approximation using quadratic rational/polynomial tensor-product surfaces $R(s,t)$ and $Q(u,v)$ with 4 by 2 patches (in θ-direction and in ϕ-direction), as shown in Figs. 4(b)–(c), have the error bound as

$$d_H(\mathbf{H},R) \leqslant 0.0331 \quad \text{and} \quad d_H(\mathbf{H},Q) \leqslant 0.451.$$

Also, the error bounds for the approximations of the torus-like helicoid surface by $k_1 \times k_2$ patches of $R(t,s)$ and $Q(u,v)$ with $k_1 \times k_2 = 4 \times 4$, 8×2 and 8×4, are obtained as shown in Table 2.

5. Comments

In this paper we presented the approximation method of the cylindrical helix by conic, quadratic Bézier curve, biconic and biquadratic Bézier curve. For each case we presented the error bound of the Haus-

Table 2
The error bounds of $d_H(\mathbf{H}, R)$ and $d_H(\mathbf{H}, Q)$ for the given torus-like helicoid surface $\mathbf{H}(\theta, \phi)$, $(\theta, \phi) \in [0, 2\pi] \times [0, \pi]$ when $p = \rho = 1$ and $r = 5$, using $k_1 \times k_2$-patches of the approximation surfaces for $k_1 \times k_2 = 4 \times 2$, 4×4, 8×2 and 8×4

No. patches	$d_H(\mathbf{H}, R)$	$d_H(\mathbf{H}, Q)$
4×2	3.31×10^{-2}	4.51×10^{-1}
4×4	3.31×10^{-2}	3.70×10^{-1}
8×2	3.95×10^{-3}	8.49×10^{-2}
8×4	3.95×10^{-3}	2.26×10^{-2}

dorff distance between the helix and each approximation curve. We also showed that all approximation methods yield G^1 conic and G^1 quadratic splines, and have the error bounds which are of approximation order three and monotone increasing with respect to the length of the helix. Using our method of helix approximation, we presented the torus-like helicoid approximation by quadric surfaces and quadratic Bézier tensor product surfaces. Using the Floater's error analysis (Floater, 1995), we presented the error bounds for the surface approximations. Although torus-like helicoid is approximated in this paper, any sweeping surface of conic section along the helix can be also approximated by quadric surfaces and quadratic Bézier tensor product surfaces by the same method proposed in this paper.

To match the tangent direction of helix and quadratic rational/polynomial approximation at both end points the bi-quadratic rational/polynomial approximation is needed. The error bound analysis for the bi-quadratic rational/polynomial approximation can be obtained by the same method of the error bound analysis in this paper.

Acknowledgements

The authors are very grateful to the anonymous referees for their valuable suggestions. This study was supported by research funds from Chosun University, 2005.

Appendix A

Proof of Proposition 4. Using the chain rule for the multi-variables function we have

$$pE'(\alpha) = \frac{\partial \varepsilon(t_A)}{\partial \alpha} = \frac{\partial \varepsilon}{\partial \alpha}\bigg|_{t=t_A} + \varepsilon'(t_A)\frac{\partial t_A}{\partial \alpha}.$$

Since $\varepsilon'(t_A) = 0$, we have

$$pE'(\alpha) = \frac{\partial \varepsilon}{\partial \alpha}\bigg|_{t=t_A} = \frac{p(xy_\alpha - x_\alpha y) - r^2(z_\alpha w - z w_\alpha)}{r^2 w^2}\bigg|_{t=t_A},$$

where the subscripts mean partial derivatives. By simple calculations, we have

$$pE'(\alpha) = \frac{2p\alpha \sin\alpha(1-2t_A)t_A(1-t_A)}{w(t_A)^2} > 0$$

since $0 < t_A < 1/2$. Thus the upper bounds (3) and (4) of $d_H(\mathbf{h}, \mathbf{r})$ and $d_H(\mathbf{h}, \mathbf{q})$, respectively, are strictly increasing with respect to α.

By the Taylor expansion of the followings at $\alpha = 0$

$$\begin{aligned}
t_A &= \frac{\sqrt{3}-1}{2\sqrt{3}} + \frac{1}{30\sqrt{3}}\alpha^2 + \mathcal{O}(\alpha^4),\\
x(t_A) &= r - \frac{r}{3}\alpha^2 + \mathcal{O}(\alpha^4),\\
y(t_A) &= -\frac{r}{\sqrt{3}}\alpha + \frac{7r}{30\sqrt{3}}\alpha^3 + \mathcal{O}(\alpha^5),\\
z(t_A) &= -\frac{p}{\sqrt{3}}\alpha + \frac{p}{15\sqrt{3}}\alpha^3 + \mathcal{O}(\alpha^5),\\
w(t_A) &= 1 - \frac{1}{6}\alpha^2 + \mathcal{O}(\alpha^4),\\
\frac{y(t_A)}{x(t_A)} &= \frac{-(r/\sqrt{3})\alpha + (7r/30\sqrt{3})\alpha^3 + \mathcal{O}(\alpha^5)}{r - (r/3)\alpha^2 + \mathcal{O}(\alpha^4)} = -\frac{1}{\sqrt{3}}\alpha - \frac{1}{10\sqrt{3}}\alpha^3 + \mathcal{O}(\alpha^5),\\
\frac{z(t_A)}{w(t_A)} &= \frac{-(p/\sqrt{3})\alpha + (p/15\sqrt{3})\alpha^3 + \mathcal{O}(\alpha^5)}{1 - (1/6)\alpha^2 + \mathcal{O}(\alpha^4)} = -\frac{p}{\sqrt{3}}\alpha - \frac{p}{10\sqrt{3}}\alpha^3 + \mathcal{O}(\alpha^5),
\end{aligned}$$

we have

$$E(\alpha) = \left\{\frac{y(t_A)}{x(t_A)} - \frac{1}{3}\left(\frac{y(t_A)}{x(t_A)}\right)^3 + \cdots\right\} - \frac{z(t_A)}{pw(t_A)} = \frac{1}{9\sqrt{3}}\alpha^3 + \mathcal{O}(\alpha^5).$$

Thus the upper bounds (3) and (4) of $d_H(\mathbf{h}, \mathbf{r})$ and $d_H(\mathbf{h}, \mathbf{q})$, respectively, have the approximation order three $\mathcal{O}(\alpha^3)$. □

References

Ahn, Y.J., 2001. Conic approximation of planar curves. Computer-Aided Design 33 (12), 867–872.

Ahn, Y.J., 2002a. Geometric conic spline approximation in CAGD. Comm. Korean Math. Soc. 17 (2), 331–347.

Ahn, Y.J., 2002b. Error bound analysis for cubic approximation of conic section. Comm. Korean Math. Soc. 17 (4), 741–754.

Ahn, Y.J., Kim, H.O., 1997. Approximation of circular arcs by Bézier curves. J. Comput. Appl. Math. 81, 145–163.

Ahn, Y.J., Kim, H.O., 1998. Curvatures of the quadratic rational Bézier curves. Comput. Math. Appl. 36 (9), 71–83.

de Boor, C., Höllig, K., Sabin, M., 1987. High accuracy geometric Hermite interpolation. Computer Aided Geometric Design 4, 169–178.

Cox, M.G., Harris, P.M., 1990. The approximation of a composite Bézier cubic curve by a composite Bézier quadratic curve. IMA J. Numer. Anal. 11, 159–180.

Degen, W.L.F., 1992. Best approximations of parametric curves by spline. In: Lyche, T., Schumaker, L.L. (Eds.), Mathematical Methods in CAGD II. Academic Press, New York, pp. 171–184.

Degen, W.L.F., 1993. High accurate rational approximation of parametric curves. Computer Aided Geometric Design 10, 293–313.

Dokken, T., Dæhlen, M., Lyche, T., Mørken, K., 1990. Good approximation of circles by curvature-continuous Bézier curves. Computer Aided Geometric Design 7, 33–41.
Farin, G., 1989. Curvature continuity and offsets for piecewise conics. ACM Trans. Graph. 8 (2), 89–99.
Farin, G., 1998. Curves and Surfaces for Computer Aided Geometric Design. Academic Press, San Diego, CA.
Floater, M., 1995. High order approximation of conic sectons by quadratic splines. Computer Aided Geometric Design 12, 617–637.
Floater, M., 1997. An $\mathcal{O}(h^{2n})$ Hermite approximation for conic sectons. Computer Aided Geometric Design 14, 135–151.
Goldapp, M., 1991. Approximation of circular arcs by cubic polynomials. Computer Aided Geometric Design 8, 227–238.
Höllig, K., Koch, J., 1995. Geometric Hermite interpolation. Computer Aided Geometric Design 12, 567–580.
Höllig, K., Koch, J., 1996. Geometric Hermite interpolation with maximal order and smoothness. Computer Aided Geometric Design 13, 681–696.
Jehárusz, I., 1995. Approximating the helix with rational cubic Bézier curves. Computer-Aided Design 27, 587–593.
Lee, E.T., 1987. The rational Bézier representation for conics. In: Geometric modeling: Algorithms and New Trends, Philadelphia. SIAM, Academic Press, pp. 3–19.
Mick, S., Röschel, O., 1990. Interpolation of helical patches by kinematics rational Bézier patches. Computers and Graphics 14 (2), 275–280.
Mørken, K., 1990. Best approximation of circle segments by quadratic Bézier curves. In: Laurent, P.J., Le Méhauté, A., Schumaker, L.L. (Eds.), Curves and Surfaces. Academic Press, New York.
Pavlidis, T., 1983. Curve fitting with conic splines. ACM Trans. Graph. 2, 1–31.
Piegl, L., 1986. The sphere as a rational Bézier surfaces. Computer Aided Geometric Design 3, 45–52.
Piegl, L., 1987. On the use of infinite control points in CAGD. Computer Aided Geometric Design 4, 155–166.
Piegl, L., Tiller, W., 1987. Curve and surface constructions using rational B-splines. Computer-Aided Design 19 (9), 485–498.
Pratt, V., 1985. Techniques for conic splines. In: Proceedings of SIGGRAPH 85. ACM, New York, pp. 151–159.
Schaback, R., 1993. Planar curve interpolation by piecewise conics of arbitrary type. Constructive Approximation 9, 373–389.
Sederberg, T., Anderson, D., Goldman, R., 1985. Implicit representation of parametric curves and surfaces. Computer Vision Graphic Image Proc. 28, 72–84.
Seemann, G., 1997. Approximating a helix segment with a rational Bézier curve. Computer Aided Geometric Design 14, 475–490.
Tiller, W., 1983. Rational B-splines for curve and surface representation. IEEE Computer Graph. Appl. 3 (6), 61–69.
Wilson, P.R., 1987. Conic representations for sphere description. IEEE Computer Graph. Appl. 7 (4), 1–31.
Yang, X., 2003. High accuracy approximation of helices by quintic curves. Computer Aided Geometric Design 20, 303–317.